

Alteration of gut microbiota by vancomycin and bacitracin improves insulin resistance *via* glucagon-like peptide 1 in diet-induced obesity

Injae Hwang,^{*,1} Yoon Jeong Park,^{†,1} Yeon-Ran Kim,^{*} Yo Na Kim,[‡] Sojeong Ka,^{*} Ho Young Lee,[§] Je Kyung Seong,[‡] Yeong-Jae Seok,^{*,†} and Jae Bum Kim^{*,2}

^{*}Department of Biological Sciences, Institute of Molecular Biology and Genetics, [†]Department of Biophysics and Chemical Biology, [‡]College of Veterinary Medicine, and [§]College of Medicine, Seoul National University, Seoul, Korea

ABSTRACT Firmicutes and Bacteroidetes, 2 major phyla of gut microbiota, are involved in lipid and bile acid metabolism to maintain systemic energy homeostasis in host. Recently, accumulating evidence has suggested that dietary changes promptly induce the alteration of abundance of both Firmicutes and Bacteroidetes in obesity and its related metabolic diseases. Nevertheless, the metabolic roles of Firmicutes and Bacteroidetes on such disease states remain unclear. The aim of this study was to determine the effects of antibiotic-induced depletion of Firmicutes and Bacteroidetes on dysregulation of energy homeostasis in obesity. Treatment of C57BL/6J mice with the antibiotics (vancomycin [V] and bacitracin [B]), in the drinking water, before diet-induced obesity (DIO) greatly decreased both Firmicutes and Bacteroidetes in the gut as revealed by pyrosequencing of the microbial 16S rRNA gene. Concomitantly, systemic glucose intolerance, hyperinsulinemia, and insulin resistance in DIO were ameliorated *via* augmentation of GLP-1 secretion (active form; 2.03-fold, total form; 5.09-fold) independently of obesity as compared with untreated DIO controls. Furthermore, there were increases in metabolically beneficial metabolites derived from the gut. Together, our data suggest that Firmicutes and Bacteroidetes potentially mediate insulin resistance through modulation of GLP-1 secretion in obesity.—Hwang, I., Park, Y. J., Kim, Y. -R., Kim, Y. N., Ka, S., Lee, H. Y., Seong, J. K., Seok, Y.-J., Kim, J. B. Alteration of gut microbiota by vancomycin and bacitracin improves insulin resistance *via* glucagon-like peptide 1 in diet-induced obesity. *FASEBJ*, 29, 2397–2411 (2015). www.fasebj.org

Key Words: gut hormone · insulin sensitivity · metabolites

OBESITY AND OBESITY-RELATED metabolic diseases including cancer, type 2 diabetes, and cardiovascular diseases impose a high social burden in terms of quality of life (1–3). Many

groups have investigated the effects of genetic and environmental factors on the development of obesity and demonstrated that several factors such as adipose tissue inflammation and hepatic lipid metabolism are associated with the etiology of obesity (4, 5).

A number of studies suggest that gut microbiota is closely linked to adiposity, insulin sensitivity, and glucose metabolism (6, 7). Studies performed in germ-free mice, which are resistant to DIO, suggested that gut microbiota plays a key role in the regulation of adiposity and host energy homeostasis (6, 8). Furthermore, modulation of gut microbiota with the antibiotic treatment leads to reduction of glucose intolerance, adiposity, and adipose tissue inflammation (9). For instance, treatment of a combination of norfloxacin and ampicillin to obese mice resulted in a decrease in the number of cecal aerobic and anaerobic bacteria followed by improved glucose tolerance and liver lipid metabolism independently of obesity (10). Among the various phyla in the gut, it has been noted that a shift in the abundance of 2 major phyla, Firmicutes and Bacteroidetes, correlates with the development of obesity (7, 11). In genetically obese *ob/ob* mice, the development of obesity is associated with a reduction in the abundance of Bacteroidetes and a proportional increase in Firmicutes (7). Moreover, analogous differences in gut microbiota have been reported in studies of lean *versus* obese humans (12). However, accumulating evidence has suggested that there is no correlation between the proportions of Firmicutes and Bacteroidetes and obesity (13, 14). Schwartz *et al.* reported that there is more Bacteroidetes in the gut of overweight and obese humans as compared with lean humans (13). Another group also suggested that higher abundance of Firmicutes is present in lean people relative to obese people (14). Therefore, there is controversy regarding changes in the relative abundance of Firmicutes and Bacteroidetes in gut microbiota are related to obesity. Intriguingly, Firmicutes and Bacteroidetes have been

Abbreviations: Ab-NH, antibiotics-treated normal chow to high-fat diet transited; B, bacitracin; CE-MS, capillary ethanol mass spectrometry; DIO, diet-induced obesity; EAT, epididymal adipose tissue; Ex(9-39), exendin 9-39 amide; GLP, glucagon-like peptide; H-89, H-89 dihydrochloride hydrate; HFD, high-fat diet; IAT, inguinal adipose tissue; LBM, lean body mass; NC, normal chow-fed; NH, normal chow to high-fat diet transited; SVC, stromal vascular cell; TCA, taurocholic acid; V, vancomycin

¹ These authors contributed equally to this work.

² Correspondence: Department of Biological Sciences, Institute of Molecular Biology and Genetics, Seoul National University, 1 Gwanak-ro, Gwanak-gu, Seoul 151-742, Korea. E-mail: jaebkim@snu.ac.kr
doi: 10.1096/fj.14-265983

implicated in the regulation of lipid and bile acid metabolism, maintaining energy homeostasis in the host (15–17). Particularly, both phyla are enriched with genes encoding multiple enzymes that govern carbohydrate and lipid metabolism (15). In addition, both Firmicutes and Bacteroidetes promptly engage in the regulation of bile acid modification and govern bile acid-controlled endocrine functions including triglyceride, cholesterol, and glucose homeostasis (16). Importantly, it has been demonstrated that perturbations of bile acid-mediated signaling pathway influence risk of metabolic complications such as obesity and diabetes (17). Despite such common features shared by Firmicutes and Bacteroidetes, it has not been precisely elucidated the possible roles of Firmicutes and Bacteroidetes in dysregulation of energy homeostasis in obesity and its related disorder.

Gut hormones, glucose-dependent insulinotropic polypeptide, glucagon-like peptide (GLP)-1 and -2, are crucial regulators of processes that contribute to whole-body energy metabolism, including satiety, gut motility, insulin secretion, and glucose uptake (18). Among the 3 hormones, GLP-1 is known to have antidiabetic effects and is secreted by several cell types such as L-cells in the posterior gut tract and neurons in the brain (19, 20). Although short chain fatty acids produced by certain types of gut microbiota stimulate GLP-1 secretion through G-protein-coupled receptor signaling (21), it is largely unknown whether changes in gut microbiota in response to nutrient cues would modulate GLP-1 secretion.

In this study, we demonstrated that treatment with the antibiotics, V and B, before DIO depleted Firmicutes and Bacteroidetes in the gut and ameliorated insulin resistance. Notably, we found that such beneficial effect on systemic energy homeostasis in the host was mediated by stimulation of GLP-1 secretion. Furthermore, there were increments of gut metabolites, which positively regulate host energy metabolism.

MATERIALS AND METHODS

Animal experiments

C57BL/6J mice were obtained from Central Lab Animal Inc. (Seoul, South Korea) and were housed in colony cages under a 12-hour light-dark cycle with free access to food and water. Mice were allowed to acclimate for 2 weeks before the study. To assess the impact of antimicrobial strategies on metabolic changes in DIO mice, 8-week-old male mice were fed normal chow for 4 weeks and then fed a high-fat diet (HFD) for 4 weeks [normal chow to high-fat diet transited (NH) group]. For mice with changes in gut microbiota [antibiotics-treated normal chow to HFD transited (Ab-NH) group], these mice were administered drinking water containing V hydrochloride (0.5 g/L; v2002; Sigma-Aldrich, St. Louis, MO, USA) and B zinc salt (1.0 g/L; B5150; Sigma-Aldrich). After 4 weeks, NH and Ab-NH mice were switched from a normal chow to a HFD comprising 60% kilocalories from fat composed of soybean oil and lard (Research Diets Inc., New Brunswick, NJ, USA). Ab-NH group continued to receive water with V + B. Age-matched normal chow-fed (NC) mice were maintained without antibiotics (V + B) and HFD. In the experimental set, glucose tolerance tests, insulin tolerance tests, and plasma insulin measurements were performed for each group (NC, NH, and Ab-NH groups). After 2 weeks of

recovery, on the day of killing, various metabolic parameters of the Ab-NH group were compared with the NC and NH groups. Each experimental group used 3 to 10 mice. All experiments were approved by the Seoul National University Institutional Animal Care and Use Committees.

Body weight, food intake, and water consumption

Body weight, food intake, and water consumption were measured every week after the start of antibiotics or HFD treatment during the indicated time periods. Pre-measured amounts of food were placed in the cage. After 24 hours, food was reweighed and the amount of consumed food was calculated by difference. The average food consumption was calculated from 4 repeated experiments. To measure water consumption, the volume of water consumed was quantified once a week for 8 weeks after the start of antibiotics (V + B) administration. Water (100 ml) with or without antibiotics was provided in a sterile bottle. After 24 hours, the remaining water was measured by mass cylinder.

Pyrosequencing data analyses

The basic analyses were performed on cecal contents according to procedures described in other studies (22). The obtained reads from the different samples were sorted by the unique barcodes of each PCR product. The sequences of the bar code, linker, and primers were removed from the original sequencing reads. Any reads containing 2 or more ambiguous nucleotides, a low-quality score (average score < 25), or reads shorter than 300 bp were discarded. The taxonomic classification of each read was assigned using the EzTaxon-e database (<http://eztaxon-e.ezbiocloud.net>), which contains the 16S rRNA gene sequence of type strains that have valid published names and representative species-level phylotypes of either cultured or uncultured entries in the GenBank database with complete hierarchical taxonomic classification from the phylum to species level (23). This experiment was performed at Chunlab Inc. (Seoul, South Korea).

Glucose tolerance test

As described previously (24), after 7 hours of food withdrawal, mice were administered a glucose solution (2 g/kg glucose, 20% glucose solution) through intraperitoneal injections or oral gavages. Blood samples were collected at 15, 30, 60, 90, 120, and 150 minutes after injection and blood glucose level was measured. For exendin 9-39 amide [Ex(9-39)] injection study using NH and Ab-NH mice, these groups were intraperitoneally injected with either glucose alone or glucose mixed with Ex(9-39) (25 nmol/kg; ab141101; Abcam, Cambridge, United Kingdom). Glucose tolerance test was performed by intraperitoneal injection of glucose at 2 g/kg body weight, followed by measurement of blood glucose at 0, 15, 30, 45, 60, 75, 90, and 120 minutes after intraperitoneal injection.

Insulin tolerance test

As described previously (24), after 7 hours of food withdrawal, mice were injected with insulin (I-5500; Sigma-Aldrich) *via* the peritoneal cavity at a dose of 0.4 U/kg. Blood was sampled at 15, 30, 60, 90, and 120 minutes after injection by drawing 3 μ L of blood from the tip of the tail vein.

Western blot analyses

Muscle tissues and livers isolated from each mice were homogenized with modified immunoprecipitation assay buffer [50 mM

Tris-HCl (pH 7.4), 150 mM NaCl, 1 mM EDTA, 1 mM PMSF, 1% (v/v) Nonidet P-40, 0.25% (w/v) Na-deoxycholate, and protease inhibitor cocktail with 1 mM NaF and 10 mM Na_3VO_4 as phosphatase inhibitors] and subjected to 8% SDS-PAGE. As previously described (25), membranes were blotted with antibodies against the following proteins: phospho-Akt (Ser473) (Cell Signaling Technology, Beverly, MA, USA), Akt (Cell Signaling Technology), phospho-GSK3 β (Ser9) (Cell Signaling Technology), GSK3 β (BD Biosciences, San Jose, CA, USA), GAPDH (AbFrontier, Gasan-dong, Seoul, Korea), and β -actin (Sigma-Aldrich).

RNA isolation and quantitative real-time PCR

As described previously (24, 25), each tissue was homogenized with TRI Reagent (Molecular Research Center, Cincinnati, OH, USA). cDNA was synthesized using M-MuLV reverse transcriptase (Fermentas, Glen Burnie, MD, USA). Q-RT-PCR was performed using the MyiQ quantitative real-time PCR detection system (Bio-Rad Laboratories, Inc.) with SYBR Green I (BioWhittaker Molecular Applications; Rockland, ME, USA). The level of each mRNA was normalized to the level of 18S rRNA or cyclophilin mRNA. The primer sequences are available upon request.

Microcomputed tomography image acquisition

Each mouse was maintained under anesthesia with isoflurane (2.5% flow rate) for the duration of the scan. Animals were positioned prone in the standard mouse bed. Limbs were positioned lateral to the body to acquire uniform computed tomography (CT) images. Whole-body CT images were acquired with a micro-single-photon emission CT/CT scanner (NanoSPECT/CT, Bioscan Inc., Washington, DC, USA). For CT image acquisition, the X-ray source was set to 200 μA and 45 kVp with 0.5 mm. The CT images were reconstructed using cone-beam reconstruction with a Shepp filter with the cutoff at the Nyquist frequency and a binning factor of 4, resulting in an image matrix of $480 \times 480 \times 632$ and a voxel size of 125 μm .

Adipose tissue volume measurement and lean body mass measurement

To measure lean body mass (LBM), the weight of each mouse was measured before image acquisition. On the whole-body image, total adipose tissue and visceral adipose tissue volume were measured as reported previously (26). LBM was defined as the weight of the body excluding the weight of fat. In this study, LBM was calculated as follows: $\text{LBM} = \{\text{body weight (g)} - [\text{total adipose tissue volume (cm}^3) \times 0.9 \text{ (g/cm}^3)]\}$, where 0.9 g/cm³ is the density of fat. Detailed methods were described in a previous report (26).

Adipose tissue fractionation and flow cytometry analyses

Adipose tissue was fractionated as previously described (27). Briefly, epididymal adipose tissues (EATs) were weighed, chopped, and incubated in collagenase buffer for 30 minutes at 37°C with shaking. After centrifugation, adipocytes in the supernatant were removed. The pelleted stromal vascular cell (SVC) fraction was used for flow cytometry. Adipose tissue SVC pellets were incubated with red blood cell lysis buffer [a 1:9 mixture of 0.17 M Tris (pH 7.65) and 0.16 M NH_4Cl], centrifuged at 1300 rpm for 5 minutes, and resuspended in PBS. For macrophage analyses, SVCs were stained with CD11b (BD Bioscience, San Jose, CA, USA), F4/80 (eBioscience, San Diego, CA, USA), and CD11c

(eBioscience) monoclonal antibodies for 30 minutes at 4°C. Cells were gently washed with and resuspended in PBS. SVCs were analyzed using a fluorescence-activated cell sorter Canto II (BD Bioscience).

Gut permeability test *in vivo*

This examination is based on the intestinal permeability to 4000-Da fluorescent-dextran (46944; Sigma-Aldrich) as previously described (9). After 4 hours of food withdrawal, mice were orally administered with FITC-dextran (600 mg/kg body weight, 125 mg/ml). After 1 hour, 300 μl of the blood were collected from the heart. The blood were centrifuged at 4°C, 6000 rpm, for 10 minutes. Collected serums were diluted with same volume of PBS and analyzed for FITC concentration at excitation wavelength of 485 nm and the emission wavelength of 535 nm. Standard curves of the FITC-dextran concentration were obtained by continuous diluting FITC-dextran solution with PBS (0–12.5 $\mu\text{g/ml}$).

Liver triglyceride measurement

Liver triglycerides were measured according to the manufacturer's protocol (Bioassay Systems, Hayward, CA, USA). Liver tissue samples (90–120 mg) were homogenized in 500 μl of 5% Triton X-100 with a tissue homogenizer. Total tissue extracts were incubated in a water bath to 80°C and cooled to room temperature. This step was repeated. After centrifugation of the total tissue extract, the supernatant was collected and measured optical density at 570 nm using a spectrophotometer (infinite M200; TECAN, Männedorf, Switzerland) in 96-well plates as previously described (5).

Cell culture experiments

NCI-H716 L-cell line was kindly provided by Dr. Young Min Cho (Seoul National University). Cells were grown in suspension in RPMI-1640 medium supplemented with 10% fetal bovine serum. Cells were treated with fresh medium every 2–3 days at a 1:3 dilution. NCI-H716 cells were seeded in 24-well plates (10^5 cells, 1 ml per 1 well) with fresh RPMI-1640 medium without serum supplementation. To test GLP-1 secretion, NCI-H716 cells were treated with or without taurocholic acid (TCA) sodium salt hydrate (1 mM; T4009; Sigma-Aldrich), putrescine dihydrochloride (1 mM; P5780; Sigma-Aldrich) and creatine monohydrate (1 mM; C3630; Sigma-Aldrich) followed by 2 hours incubation. H-89 dihydrochloride hydrate (H-89) (40 μM ; B1427; Sigma-Aldrich) was either treated alone or cotreated with TCA sodium salt hydrate for 2 hours incubation. Each conditioned medium from cells treated with different metabolites was carefully harvested and centrifuged. Supernatant (200 μl) was collected for GLP-1 measurement as described below.

Biochemical analyses for metabolic markers

Serum insulin, endotoxin, TNF- α , and cholesterol were measured using a mouse insulin ELISA kit (AKRIN-011T; Shibayagi, Gunma Pref., Japan), ToxinSensor Chromogenic Endotoxin Assay Kit (L00350; Genscript, Piscataway, NJ, USA), mouse TNF- α detection kit (KMC3011; Invitrogen, Carlsbad, CA, USA), and cholesterol detection reagent (TR13421; Thermo Scientific, Waltham, MA, USA), respectively, following the manufacturers' instructions. Active GLP-1 and total GLP-1 in serum were measured using GLP-1 ELISA (Active 7-36) (43-GPIHU-E01; ALPCO, Salem, NH, USA) and total GLP-1 (7-36, 9-36) ELISA

(43-GPTHU-E01; ALPCO), respectively. To measure endotoxin, serums were diluted in PBS 1/50 to 1/100 ratio (v/v). For measurement of the GLP-1 active form, glucose solution (2 g/kg) was administered to mice by oral gavage. Mice rested 30 minutes before killing and blood collection. To inhibit dipeptidyl peptidase IV activity, blood samples were placed in BD P700 tubes containing dipeptidyl peptidase IV inhibitors (BD Bioscience) immediately. Blood samples were centrifuged at 2500 rpm for 10 minutes at 4°C to isolate serum. Serum samples were used for measurement of active GLP-1 in samples that were never frozen.

Immunohistochemistry

After isolation from NC, NH, and Ab-NH mice, ileums were dissected and washed with PBS (0.1 M). They were then fixed with 10% neutral buffered formalin overnight at room temperature. After dehydration with a graded alcohol series and clearing, tissues were embedded in paraffin. Tissue sections were cut to a thickness of 4 μ m and were immunostained with anti-rabbit GLP-1 antibody (1:1000; Abcam). Before heat-induced antigen retrieval with Tris-EDTA, pH 9.0 (Thermo-Scientific, Rockford, IL, USA) for 15 min, endogenous peroxidase activity was blocked with 0.3% H₂O₂ in methanol. Sections were blocked in normal goat serum and incubated in primary antibody overnight at 4°C. They were then incubated in Alexa Fluor 488 donkey anti-rabbit IgG (1:300; Invitrogen) for 2 hours at room temperature and mounted in Vectashield containing DAPI. Immunoreactivity was visualized with a confocal microscope system (LSM 510; Carl Zeiss, Oberkochen, Germany).

Capillary ethanol-mass spectrometry-based metabolomics

Frozen ileal and cecal contents were homogenized with Dulbecco's PBS immediately after thawing. Supernatants were collected without precipitation. Supernatants (100 μ l) were centrifuged and filtered using Ultrafree-MC filter units (Millipore, Billerica, MA, USA). Samples were analyzed by capillary ethanol mass spectrometry (CE-MS) at Human Metabolome Technologies, Inc. (Yamagata, Japan). Detailed methods were described in a previous report (28).

Statistical analyses

Data are presented as the mean with SEM. Differences between 2 groups were assessed by using the Student's *t* test. Data involving more than 2 groups were analyzed by ANOVA (GraphPad Prism; GraphPad, San Diego, CA, USA). Significant ANOVA results were followed by *post hoc* tests (1-way Tukey; 2-way Bonferroni). A value of *P* < 0.05 was considered significant.

RESULTS

Treatment with V and B depletes Firmicutes and Bacteroidetes in the mouse gut

To investigate whether the modulation of intestinal microbial communities, with selective reduction of 2 major gut phyla, Firmicutes and Bacteroidetes, protects against obesity and insulin resistance, we challenged mice with antibiotics before DIO. Eight-week-old C57BL/6J male mice were fed normal chow for 4 weeks and then fed an HFD for 4 weeks (NH). As shown in **Fig. 1A**, one NH group (Ab-NH) was given free access to drinking water containing

a V + B cocktail throughout the experiment to alter the gut microbiota. V and B were selected because of their strong sterilizing effects, especially on gram-positive bacteria and anaerobes, which include major gut phyla such as Firmicutes and a considerable number of species belonging to Bacteroidetes (29–31). Moreover, V and B are minimally absorbed by the host gastrointestinal tract after oral administration (32, 33). We verified the depletion of Firmicutes and Bacteroidetes at 4 weeks of antibiotic (V + B) treatment to NC mice before HFD feeding (data not shown). In agreement with previous reports (34), there was a downward trend in the absolute abundance of gut microbiota upon HFD challenge as compared with NC group (**Fig. 1B**). Furthermore, the absolute abundance of bacterial DNA in the Ab-NH was significantly reduced relative to the NH group, suggesting that absolute richness of gut microbiota is altered by V + B. As shown in **Fig. 1C**, HFD increased the proportion of Firmicutes and decreased the proportion of Bacteroidetes compared with the populations in NC group, and V + B greatly reduced the proportions of Firmicutes and Bacteroidetes in DIO. With the substantial decrease in these phyla, the proportion of Proteobacteria increased markedly (**Fig. 1C**). Furthermore, at the class and species levels, *Escherichia coli* comprised more than half of the total bacteria (52.95%), whereas the population of EF098132_g_uc, belonging to the family Lachnospiraceae of Firmicutes, and Porphyromonadaceae_uc_s, belonging to the family Porphyromonadaceae of Bacteroidetes, decreased considerably in the Ab-NH group (**Fig. 1D**).

Gut microbiota alteration with V + B treatment ameliorates insulin resistance in DIO mice

To examine the effects of V + B-mediated modulation of gut microbiota on insulin sensitivity in DIO mice, a glucose tolerance test and an insulin tolerance test were performed. As expected, the NH group displayed impaired glucose tolerance and insulin tolerance compared with the NC group. In contrast, both of glucose and insulin intolerance were improved in the Ab-NH group as compared with the NH group (**Fig. 2A, B**). Furthermore, the serum insulin levels in the Ab-NH group were lower than those in the NH group (**Fig. 2C**). Also, upon insulin treatment, phosphorylation of Akt (Ser 473) and GSK3 β (Ser 9), 2 major components of the insulin-signaling cascade, slightly increased in the muscle and liver in the Ab-NH group (**Fig. 2D**). Because obesity-induced insulin resistance is closely associated with pancreatic islet hypertrophy (35), the size of pancreatic islets was investigated. As shown in **Fig. 2E**, treatment with V + B alleviated pancreatic islet hypertrophy in Ab-NH mice. Together, these data suggest that the prominent reduction in the abundance of Firmicutes and Bacteroidetes with V + B would ameliorate insulin resistance in DIO.

Depletion of Firmicutes and Bacteroidetes does not affect body weight gain and adiposity in DIO

Because it has been reported that the relative abundance of Firmicutes and Bacteroidetes is correlated with obesity

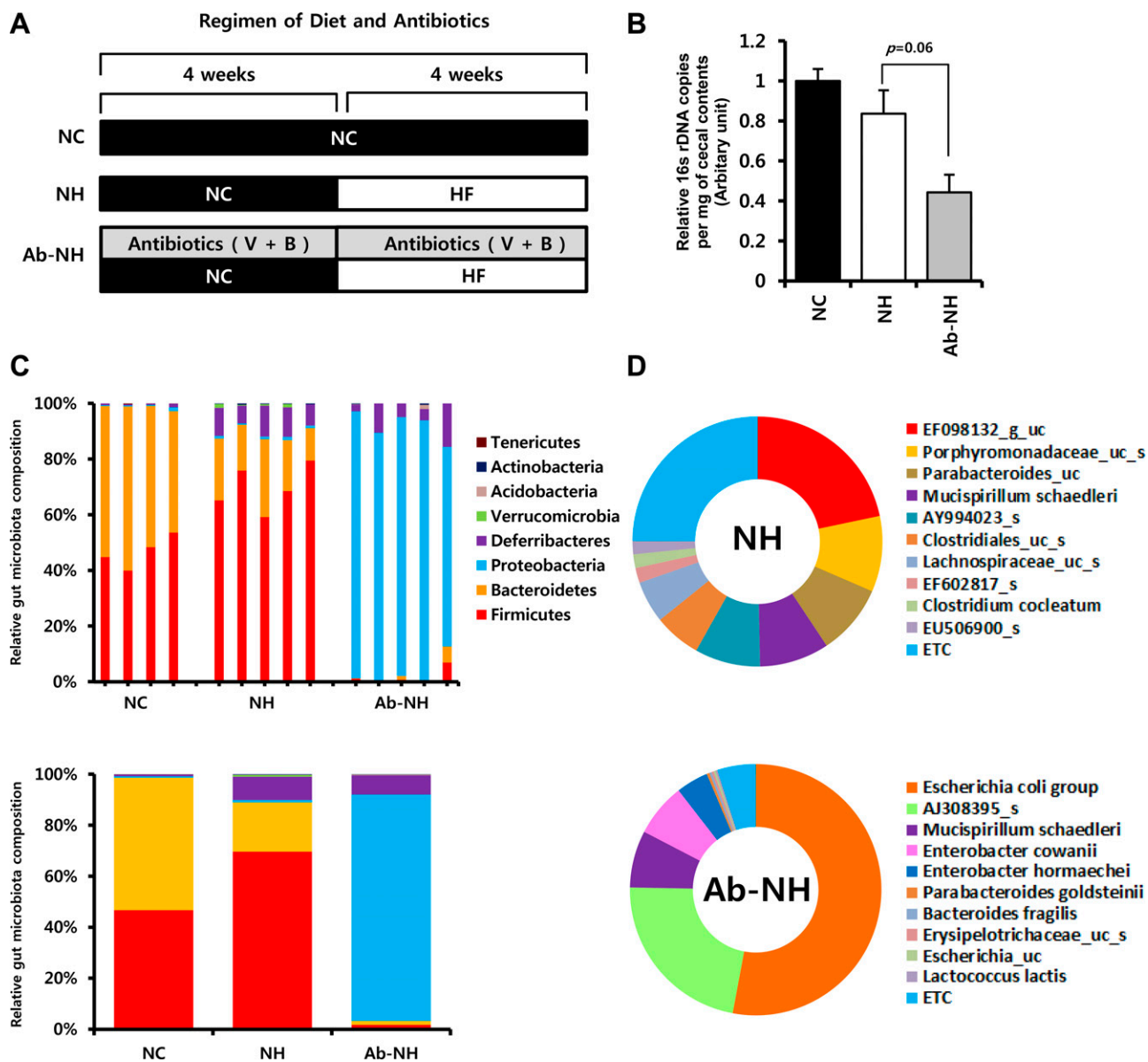


Figure 1. Experimental scheme and the population of the gut microbiota in NC, NH, and Ab-NH groups. C57BL/6J 8-week-old male mice were given drinking water with or without V + B for 4 weeks and then fed normal chow or HFD. Analyses of gut microbiota communities by 16S ribosomal DNA (rDNA) analyses from mice fed normal chow without antibiotics, an HFD without antibiotics (NH), or an HFD with antibiotics (Ab-NH). *A*) Illustration depicting the experimental strategies used in this study. Mice in the Ab-NH group were given antibiotics (0.5 g/L V with 1 g/L B; V + B) in their drinking water. After 4 weeks on a normal chow, with or without antibiotics preconditioning, mice in the NH and Ab-NH groups, respectively, were fed an HFD for another 4 weeks. Age-matched mice in the NC group were fed normal chow throughout the experimental period. *B*) Analysis of the level of 16S rDNA copies in the cecal contents. $n = 3$ per group. *C*) Bacterial 16S rDNA pyrosequencing analyses of the cecal contents of the NC, NH, and Ab-NH groups. Upper bar graphs imply gut microbiota in individual mouse and group average values are indicated in lower panel. The percentage of the community contributed by each phylum is indicated. Each phylum is denoted by a color, as shown beside the graph. *D*) Comparison of cecal microbial species compositions in NH and Ab-NH mice by 16S rDNA pyrosequencing. In the NH group, the prevalence of each species, from top to bottom, was 21.72, 9.79, 9.15, 9, 8.48, 6.07, 5.43, 1.93, 1.76, 1.73, and 24.91%. In the Ab-NH group, the prevalence of each species, from top to bottom, was 52.95, 22.35, 7.33, 6.85, 4.13, 0.36, 0.29, 0.29, 0.25, 0.25, and 4.93%. *B*) Each bar represents the mean \pm SE of the individual samples.

(6), we have asked whether depletion of Firmicutes and Bacteroidetes with V + B changed the body weight gain in DIO. Interestingly, as shown in **Fig. 3A**, body weight gain in the Ab-NH group was comparable with that in the NH group. When we examined the mass of several different fat depots, there was no significant difference between the NH and Ab-NH groups (**Fig. 3B, C**). In addition, adiposity,

abdominal fat area, whole-body fat volumes, and LBM were similar in the NH and Ab-NH groups (**Fig. 3D, E**). Furthermore, food intake and water consumption were not affected by V + B in DIO mice (**Fig. 3F, G**). These data propose that significant reduction of Firmicutes and Bacteroidetes by V + B would not be associated with obesity and adiposity.

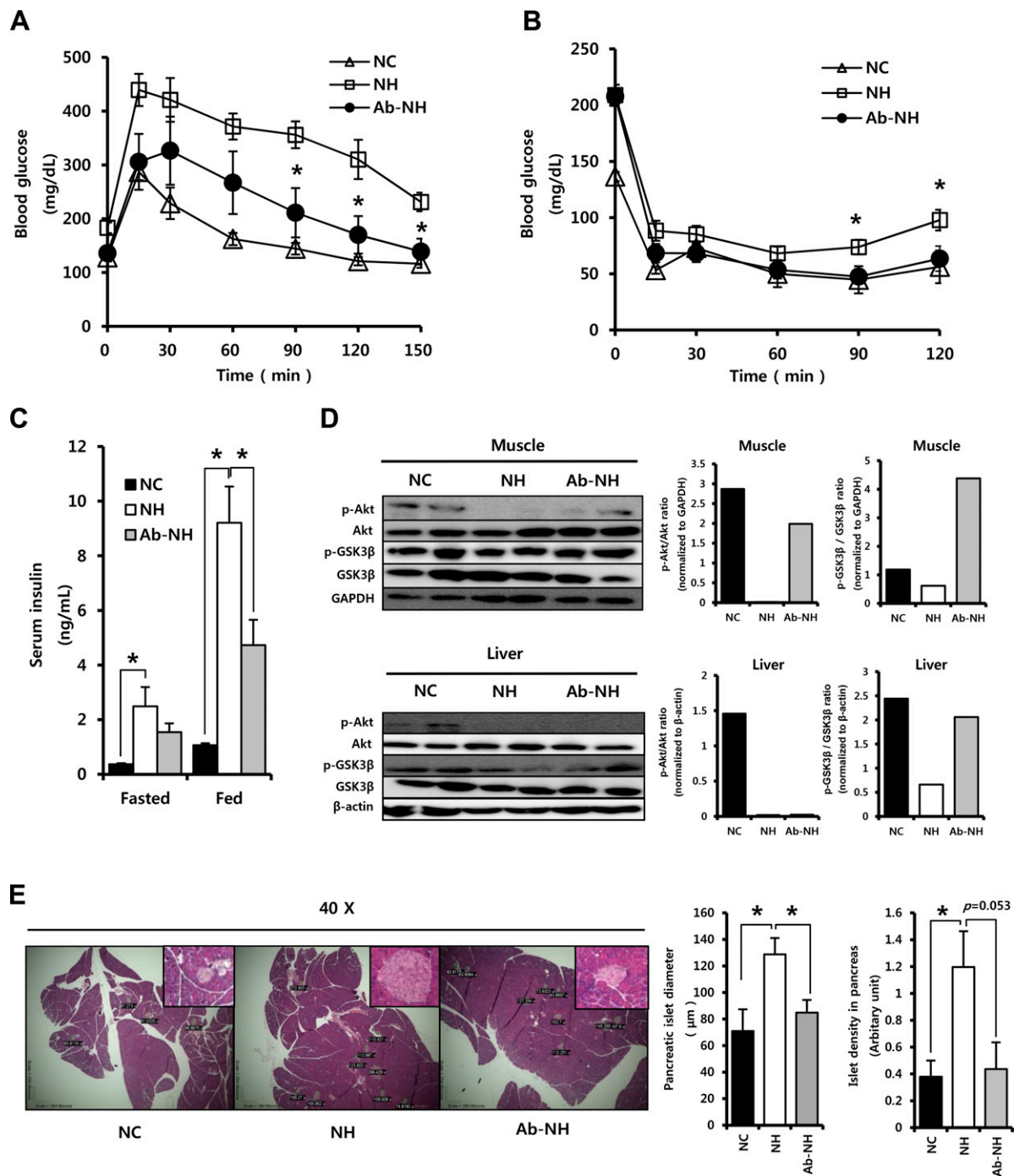


Figure 2. V + B treatment improves insulin resistance in DIO mice. *A*) At the end of the experimental period, mice were given an intraperitoneal glucose tolerance test. $n = 4$ per time point for NC group and $n = 5$ per time point for NH and Ab-NH group. *B*) The same mice tested in panel (*A*) were given an insulin tolerance test after 2 weeks of recovery. $n = 4$ per time point for NC group and $n = 5$ per time point for NH and Ab-NH groups. *C*) Blood samples were collected from the tail vein of each mouse after 7 hours of food withdrawal (“fasted” group) or normal feeding to measure the serum insulin concentration. *D*) Western blot images (left) and bar graphs (right) showing quantitative analyses of Western blot data using ImageJ (NIH, Bethesda, MD, USA) software of insulin signaling marker proteins p-Akt (s473) and p-GSK3 β (S9) in the muscle and liver. Total Akt, total GSK3 β , GAPDH in muscle and β -actin in liver were used as controls. *E*) Pancreatic islets from mice in the NC, NH, and Ab-NH groups were isolated and stained with hematoxylin and eosin. Representative images of the pancreas are shown, with enlarged images of pancreatic islets displayed in the upper right. Islet diameters (μm) ($n = 33, 31,$ and 35 for NC, NH, and Ab-NH, respectively) and density were measured by ImageJ software. *A, B, C, E*) Each bar represents the mean \pm SE of the individual samples. $*P < 0.05$.

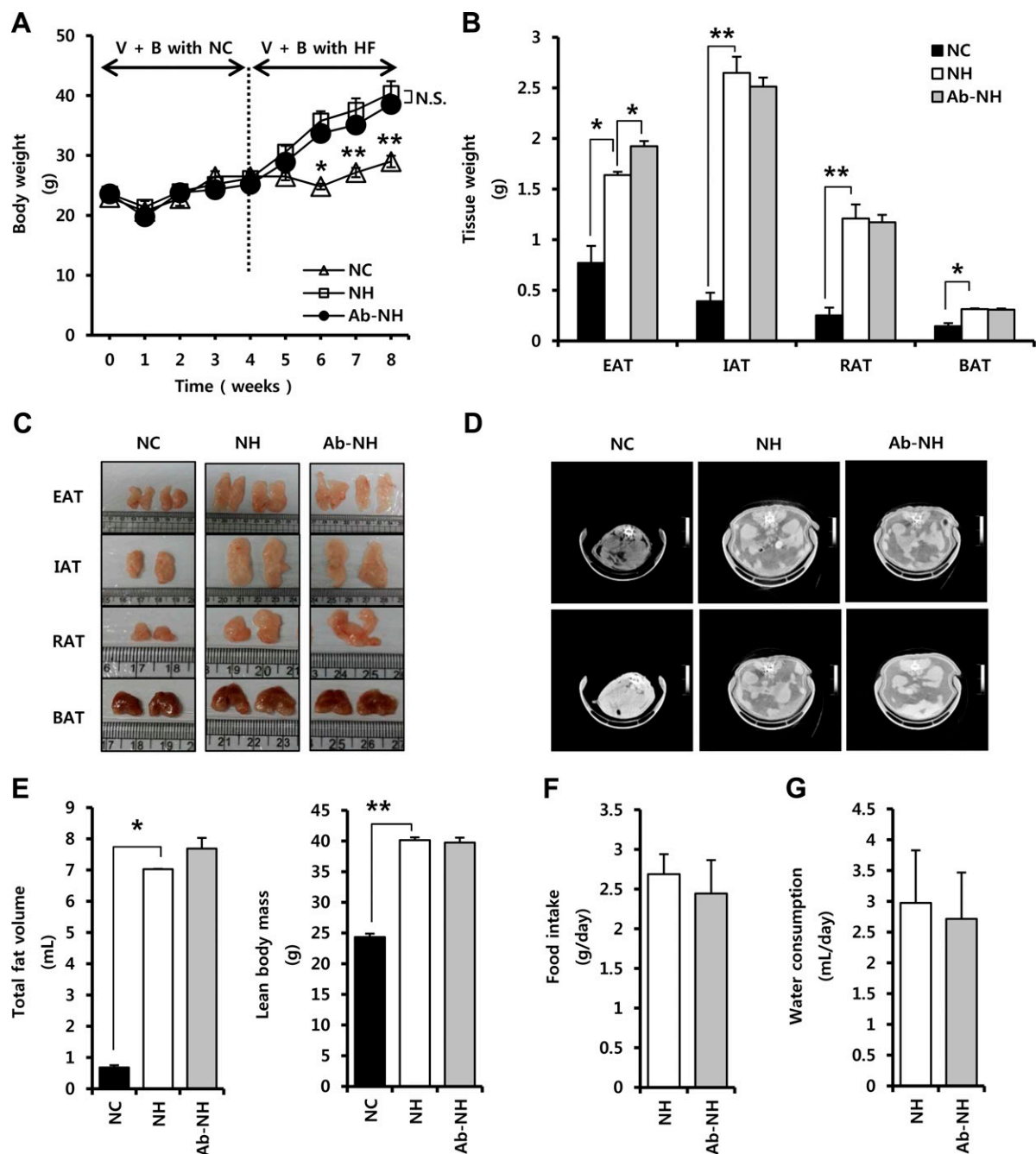


Figure 3. Body weight and body composition do not differ in NH and Ab-NH mice. *A*) Body weights were measured every week from 0 to 8 weeks during the experimental period. *Exhibits difference between NC and NH group. *B*) Major adipose tissue depots, including EAT, IAT, renal adipose tissue (RAT), and brown adipose tissue (BAT), were isolated and weighed after the experimental period. *C*) Representative images of EAT, IAT, RAT, and BAT in NC, NH, and Ab-NH are shown. Scale, 1 mm. *D*) Representative transverse cross-sectional micro-CT images of NC, NH, and Ab-NH abdominal areas. *E*) Total fat volume (left) and LBM (right) were quantified from micro-CT scans. *F*) Daily food intake was measured once a week for 8 weeks after the start of antibiotics administration to the Ab-NH group. Mice in the Ab-NH group consumed 2.85, 2.7, 3.15, 2.4, 2.05, 2.05, 2, and 2.35 g of food per day, respectively, similar to mice in the NH group. The average daily food intake over 8 weeks is shown. *G*) Water consumption was quantified once a week for 8 weeks after the start of antibiotics administration to the Ab-NH group. Water (100 ml) with or without antibiotics was provided in a sterile bottle. After 24 hours, the remaining water was measured by mass cylinder. Ab-NH mice drank 2.65, 2.75, 3.65, 2.35, 1.9, 1.9, and 2.1 ml of water in each 24-hour period sampled, similar to mice in the NH group. The average daily water consumption is shown. *A, B, E, F, G*) Each bar represents the mean \pm SE of the individual samples. N.S., not significant. * $P < 0.05$ and ** $P < 0.01$.

Reduction of Firmicutes and Bacteroidetes by V + B treatment does not affect the risk factors related to insulin resistance in DIO mice

In severe obesity, chronic adipose tissue inflammation is closely associated with insulin resistance (36, 37). In particular, an increase in proinflammatory macrophages (F4/80⁺, CD11b⁺, and CD11c⁺) in the adipose tissue of obese mice aggravates systemic insulin resistance (36). To test the hypothesis that adipose tissue inflammation contributes to improved insulin resistance in the Ab-NH group, inflammatory gene expression and macrophage infiltration were analyzed in adipose tissue. The expression of proinflammatory genes such as *Tnfα* and *Il-6* in EAT was higher in the NH and Ab-NH groups than in the NC group (Fig. 4A). Similarly, the expression of macrophage surface marker genes such as *F4/80*, *Cd11b*, and *Cd11c* was comparable in the Ab-NH and NH groups (Fig. 4A). Consistent with the changes in gene expression profiling data, the number of F4/80⁺ and CD11b⁺ macrophages in the adipose tissues of the HFD-treated groups (NH and Ab-NH) was higher than that in the NC group (Fig. 4B, C).

It is well recognized that a complex interplay between the host and the bacteria modulates systemic inflammation in obesity (38). For instance, in addition to structural imbalance and perturbation of the function of gut microbiota, disruption of gastrointestinal barrier integrity has been reported to be a critical change in the host to aggravate inflammation induced by dysbiosis of gut microbiota (9). However, there were no significant changes in the extent of gut inflammation indicated by retained expression of *Tnfα* and *Il-10* in the Ab-NH group relative to NH group (data not shown). Furthermore, the expression of the gut barrier gene *mucin 6* and tight junction genes such as *occludin (Ocln)* and *claudin 10 (Cldn10)* was not greatly different between the NH and Ab-NH group (Fig. 4D). Also, HFD-mediated elevation of gut leakage was substantially reduced in the Ab-NH group (Fig. 4E). In turn, serum endotoxin and serum TNF-α, markers of systemic inflammation, were similar in the NH and Ab-NH groups (Fig. 4F, G).

Previous studies demonstrated that dysregulation of lipid metabolism in liver was associated with obesity and its related disorders (5, 39). In the present study, the levels of serum cholesterol and hepatic triglyceride were trended upward regardless of V + B treatment upon HFD feeding indicating that HFD-induced dysregulation of lipid metabolism in the liver would not be affected by the modulation of the gut microbiota by V + B treatment (Fig. 4H, I). Thus, these results suggest that amelioration of insulin resistance in the Ab-NH group is not related with the alleviation of chronic inflammation or hepatic lipid dysregulation.

V + B-mediated alteration of gut microbiota improves glucose tolerance via stimulating GLP-1 secretion in DIO mice

GLP-1 is a prominent gut hormone that modulates whole-body insulin sensitivity (40). To investigate whether GLP-1 was involved in the improvement of insulin resistance in the Ab-NH group, serum levels of GLP-1 (7-36 amide and 9-36 amide) were measured. Intriguingly, the level of total

GLP-1 in food withdrawal status increased in the Ab-NH group to an extent comparable to NC mice (Fig. 5A). To determine whether the increase in total GLP-1 in basal status of the Ab-NH group was resulted from the different ability of L-cells to secrete GLP-1 upon glucose challenge, GLP-1 release was examined after oral glucose administration. As shown in Fig. 5B, the levels of active GLP-1 in the serum were significantly higher in the Ab-NH group than in the NH group. The reduction in active GLP-1 upon HFD feeding (Fig. 5B) is consistent with previous report that GLP-1 secretion is suppressed in obese humans (41). In addition, the degree of GLP-1 staining in the ileum increased in the Ab-NH group compared with the NH group, suggesting that the production of GLP-1 in the ileum was augmented in the Ab-NH group (Fig. 5C, D).

We next examined the involvement of GLP-1 in the enhancement of glucose tolerance in the Ab-NH group. Treatment with Ex(9-39), a well-known GLP-1 receptor antagonist, led to aggravation of glucose intolerance in NH mice relative to the NH mice treated with vehicle (Fig. 5E). Additionally, Ab-NH mice treated with Ex(9-39) exhibited significantly impaired glucose intolerance to an extent comparable to NH mice treated with Ex(9-39) (Fig. 5E). These data imply that amelioration of obesity-induced glucose intolerance in Ab-NH mice would be attributable to GLP-1-mediated beneficial effects on energy metabolism.

Modulation of 2 major phyla stimulates production of metabolically beneficial metabolites

Microbial communities actively produce various metabolites, which have the potential to affect energy homeostasis (28). As shown in Fig. 6A, B, CE-MS analyses revealed distinct gut metabolite patterns in the NH and Ab-NH groups. In contrast, serum metabolite profiles were not markedly different in the NH and Ab-NH groups (Fig. 6C, D). Among the metabolites selectively up-regulated in the Ab-NH group (Table 1), 8 metabolites including succinic acid, creatine, putrescine, sulfotyrosine, TCA, mucic acid putrescine, and 1-methylnicotinamide (Fig. 6E) were known to benefit host energy metabolism (42–49). Given previous studies reported that gut-derived metabolites are able to stimulate GLP-1 secretion (50, 51), we tested the effects of gut metabolites induced by removal of Firmicutes and Bacteroidetes on GLP-1 secretion in L-cells. Among 3 metabolites prominently induced in the Ab-NH group, TCA overtly enhanced GLP-1 secretion in L-cells, indicating that alteration of gut metabolites in Ab-NH group, in part, contributes to an increase in GLP-1 secretion in DIO (Fig. 6F). Further, protein kinase A (PKA) was appeared to be engaged in TCA-mediated GLP-1 secretion as treatment of H-89, a well-known PKA inhibitor, substantially reduced the positive effect of TCA on GLP-1 secretion (Fig. 6G). Collectively, these results suggest that depletion of Firmicutes and Bacteroidetes with V + B in DIO would alter gut metabolites and subsequently augments insulin sensitivity via increasing GLP-1 secretion.

DISCUSSION

Compelling evidences indicate that Firmicutes and Bacteroidetes, 2 major phyla of gut microbiota, play a significant

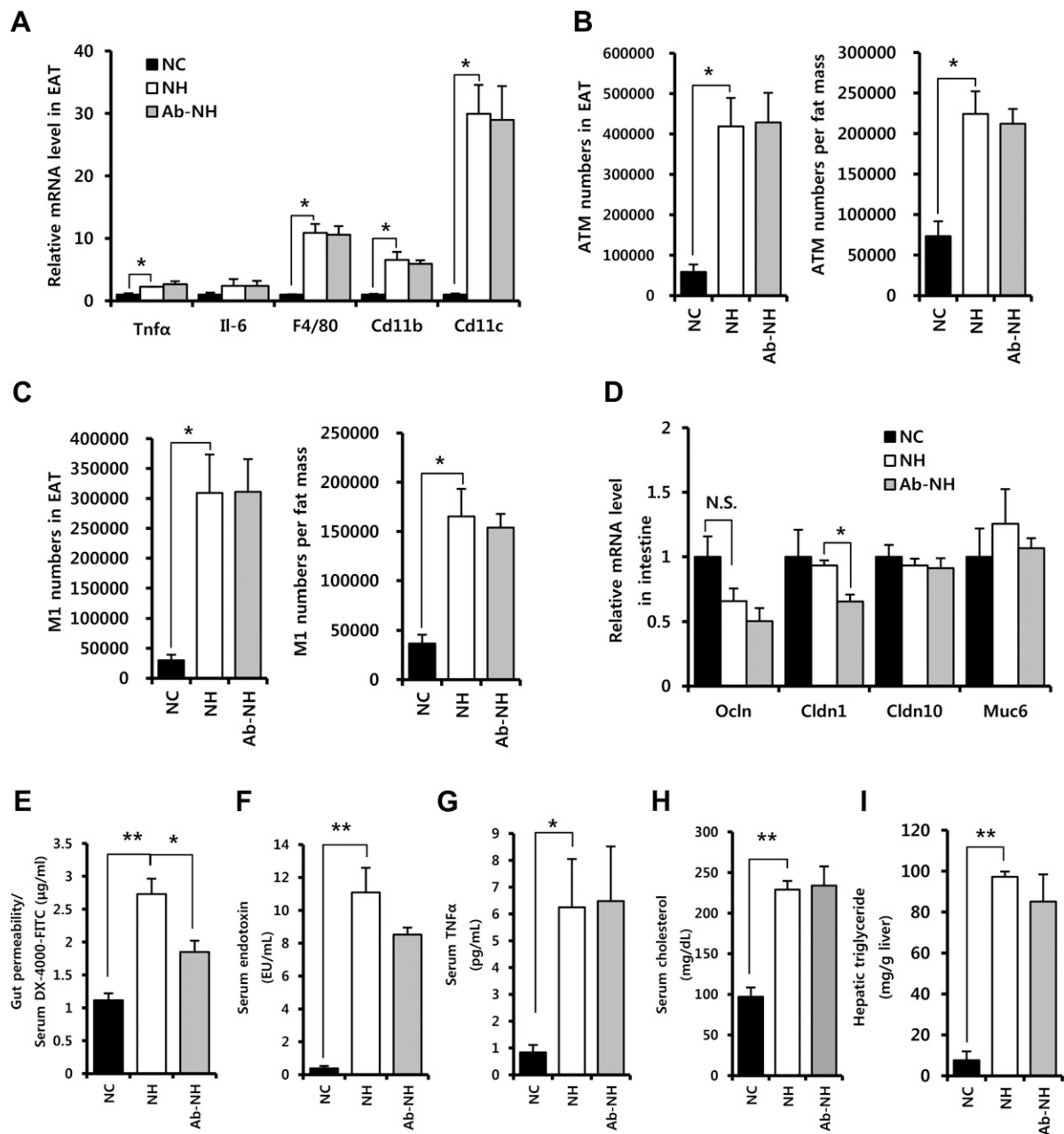


Figure 4. Adipose tissue inflammation, endotoxemia, serum cholesterol, and hepatic steatosis are not altered in Ab-NH mice. *A*) Relative mRNA levels in EAT were measured. Proinflammatory cytokines, *Tnfα* and *Il-6*, and macrophage markers, *F4/80*, *Cd11b*, and *Cd11c*, were measured by quantitative real time-PCR. *B*) Flow cytometry of adipose tissue macrophages (ATM; $F4/80^+$ and $CD11b^+$) in EAT. *C*) Flow cytometry of M1 type macrophages ($F4/80^+$, $CD11b^+$, and $CD11c^+$) in EAT. Total cell numbers are indicated in the left graph, and the number of cells per gram of adipose tissue is shown in right graph. *D*) Relative expression of gut barrier genes in the intestine: *occludin* (*Ocln*), *claudin 1* (*Cldn1*), *claudin 10* (*Cldn10*), and *Mucin 6* (*Muc6*). *E–I*) Changes in gut permeability (*E*), serum endotoxin (*F*), TNF- α (*G*), cholesterol (*H*), and hepatic triglyceride (*I*) induced by DIO were measured. $n = 5$ per group. Each bar represents the mean \pm SE of the individual samples. N.S., not significant. * $P < 0.05$ and ** $P < 0.01$.

role in the regulation of host energy metabolism (6, 9), although the association of relative abundance of Firmicutes and Bacteroidetes with obesity and its related metabolic diseases has been controversial. To elucidate the roles of Firmicutes and Bacteroidetes on obesity and its related metabolic complications, we developed a mouse model in which gut microbiota is altered by treatment with an antibiotic cocktail of V + B before the establishment of DIO. V + B treatment in DIO-altered gut microbiota, selectively by

reducing the population of Firmicutes and Bacteroidetes, and improved insulin resistance, without affecting obesity. Of note, serum GLP-1 levels and GLP-1 expression in intestinal L-cells were significantly augmented upon the V + B-mediated alteration of gut microbiota. Additionally, depletion of Firmicutes and Bacteroidetes increased production of particular metabolites in the gut, which would contribute to beneficial changes in the host energy metabolism including GLP-1 secretion. These data

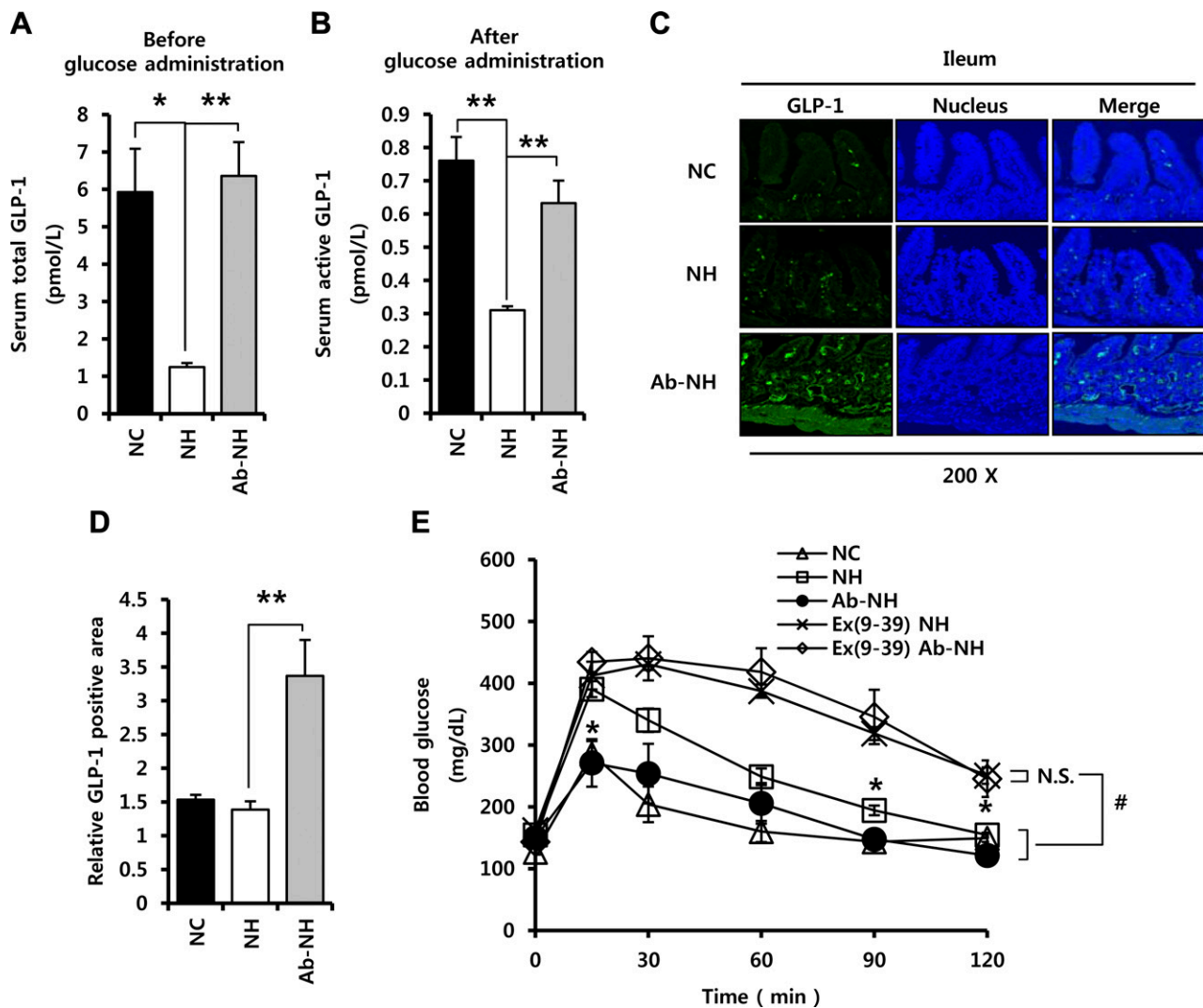


Figure 5. GLP-1 is elevated in the serum and intestinal L-cells of Ab-NH mice. *A*) Measurement of total (7-36 and 9-36 amide) GLP-1 under food withdrawal status in the NC, NH, and Ab-NH groups. $n = 5$ per group. *B*) Measurement of active (7-36 amide) GLP-1 after oral glucose administration (2 g/kg, 20% glucose solution). $n = 10$ per group. *C* and *D*) Representative immunofluorescence images of L-cells in the ileum (*C*) stained with anti-GLP-1 (green) and DAPI (blue) and quantification of the relative GLP-1-positive area (*D*). GLP-1-positive area was measured using ImageJ software. *E*) Mice were given glucose tolerance test with Ex(9-39) in the NH and Ab-NH groups. #Blood glucose levels of Ex(9-39)-treated groups showed statistical significance as compared with vehicle treated groups from 30 to 120 minutes after glucose administration. *Exhibited difference between NH and Ab-NH groups. Each bar represents the mean \pm SE of the individual samples. N.S., not significant. ** $P < 0.05$ and *** $P < 0.01$.

suggest that distinct shifts in gut microbial composition by V + B treatment would ameliorate insulin resistance in DIO by stimulating GLP-1 secretion.

Gut microbiota, particularly Firmicutes and Bacteroidetes, are involved in the control of host energy metabolism including carbohydrate, lipid, and bile acid metabolism (15, 52). More importantly, Firmicutes and Bacteroidetes share roles to regulate the response of host to dynamic changes in diets (53). Previously, it has been suggested that there is correlation between obesity and relative proportion of Firmicutes and Bacteroidetes (7). However, several lines of evidence indicated that such correlation is not always implicated in obesity and changes in the relative abundance of Firmicutes and Bacteroidetes may not be sufficient for the onset of obesity (54, 55). In present study, we observed that body weight gain and

adiposity upon HFD were not attenuated when Firmicutes and Bacteroidetes were concurrently depleted. On the other hand, we observed that obesity-induced insulin resistance was improved in parallel with the reduction in the abundance of Firmicutes and Bacteroidetes, indicating a potential role of Firmicutes and Bacteroidetes in the regulation of insulin sensitivity in DIO.

Previously, it has been reported that patients with type 2 diabetes are relatively enriched with gram-negative bacteria belonging to the phyla Bacteroidetes and Proteobacteria (56, 57). Additionally, it has been shown that such increases in gut microbiota are associated with metabolic endotoxemia through increasing plasma LPS, leading to oxidative stress, macrophage infiltration markers, and most inflammatory markers inducing insulin resistance (38). In particular, disruption of gastrointestinal barrier

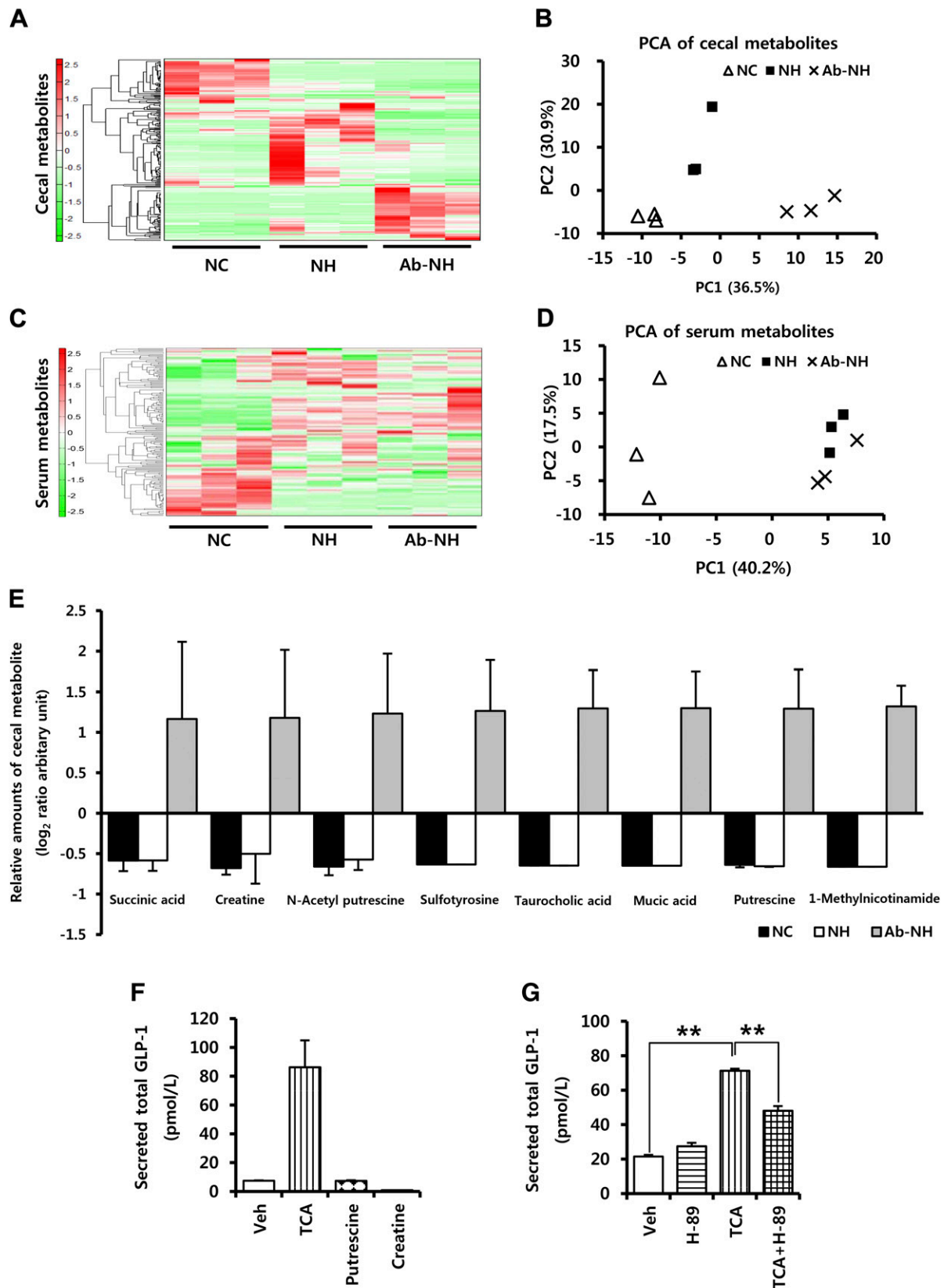


Figure 6. Analyses of gut and serum metabolites from NC, NH, and Ab-NH mice. Heat maps of the relative amounts of metabolites identified in the ileal contents (A) and serum (C) using CE-MS. $n = 3$ per group. The relative amount of each individual metabolite was indicated by color intensity: red for positive correlation and green for inverse correlation. B, D) Principal component analyses (PCA) of metabolomics results. Dispersion of metabolites identified in the ileal contents (B) and serum (D) in NC, NH, and Ab-NH groups. $n = 3$ per group. E) The cecal levels of 8 metabolites metabolically beneficial in (continued on next page)

TABLE 1. Metabolites exclusively up-regulated in the Ab-NH group

No.	Compound name	KEGG ID	Relative folds of inductions ^a			P value ^b
			NC	NH	Ab-NH	
1	Succinic acid	C00042	-0.585 ± 0.075	0.583 ± 0.075	1.167 ± 0.548	0.082969
2	Creatine	C00300	-0.679 ± 0.046	-0.501 ± 0.213	1.180 ± 0.483	0.056252
3	Pro	C00148 C00763 C16435	-0.689 ± 0.003	-0.527 ± 0.103	1.216 ± 0.455	0.05556
4	N-acetylputrescine	C02714	-0.660 ± 0.062	-0.573 ± 0.075	1.233 ± 0.426	0.0475
5	XC0065	-	-0.623	-0.623	1.246 ± 0.412	0.04535
6	Sulfotyrosine	No ID	-0.633	-0.633	1.266 ± 0.362	0.034368
7	XA0036	-	-0.634	-0.634	1.267 ± 0.359	0.033863
8	3-methyladenine	C00913	-0.638	-0.638	1.276 ± 0.335	0.029358
9	Imidazolelactic acid	C05568	-0.651	-0.625 ± 0.026	1.276 ± 0.332	0.02857
10	Glucuronic acid	C00191	-0.885	-0.380 ± 0.261	1.265 ± 0.043	0.021719
11	Putrescine	C00134	-0.638 ± 0.018	-0.655 ± 0.004	1.294 ± 0.278	0.019725
12	TCA	C05122	-0.648	-0.648	1.296 ± 0.273	0.019123
13	Homovanillic acid	C05582	-0.331 ± 0.479	-0.810	1.141 ± 0.264	0.017773
14	Mucic acid	C00879 C01807	-0.649	-0.649	1.299 ± 0.262	0.017548
15	1-pyrroline 5-carboxylic acid	C03912	-0.650	-0.650	1.300 ± 0.255	0.016711
16	1 <i>H</i> -imidazole-4-propionic acid	No ID	-0.724	-0.566 ± 0.081	1.289 ± 0.272	0.014741
17	S-hexylglutathione	C02886	-0.655	-0.655	1.310 ± 0.216	0.011908
18	N ¹ -methyl-4-pyridone -5-carboxamide	C05843	-0.655	-0.655	1.310 ± 0.214	0.011624
19	7-methylguanine	C02242	-0.740	-0.514 ± 0.226	1.254 ± 0.300	0.010997
20	XC0126	-	-0.657	-0.657	1.313 ± 0.200	0.010143
21	XA0035	-	-0.657	-0.657	1.314 ± 0.198	0.009986
22	Urea	C00086	-0.657	-0.657	1.314 ± 0.196	0.009728
23	Carboxymethyllysine	No ID	-0.503 ± 0.024	-0.789 ± 0.062	1.291 ± 0.240	0.009505
24	1-methylnicotinamide	C02918	-0.661	-0.661	1.322 ± 0.147	0.005459
25	Cadaverine	C01672	-0.722 ± 0.014	-0.602 ± 0.017	1.324 ± 0.121	0.003372
26	Gluconolactone	C00198	-0.664	-0.664	1.329 ± 0.094	0.002235
27	Creatinine	C00791	-0.760 ± 0.069	-0.547 ± 0.164	1.307 ± 0.098	0.001635
28	Gluconic acid	C00257	-0.292 ± 0.173	-0.937 ± 0.160	1.229 ± 0.204	0.001428
29	Isethionic acid (2-hydroxyethanesulfonic acid)	C05123	-0.654 ± 0.073	-0.666 ± 0.068	1.320 ± 0.130	0.000838
30	N-acetylhistidine	C02997	-0.673 ± 0.149	-0.636 ± 0.093	1.309 ± 0.128	0.000425

KEGG, Kyoto Encyclopedia of Genes and Genomes. ^aAverage ± SE, Log₂ scale, *n* = 3. ^bStudent's *t* test (NH vs. Ab-NH).

integrity appeared to cause a critical change in the host to aggravate inflammation induced by dysbiosis of the microbiome (38, 58). In the present study, there was an increase in the relative abundance of Proteobacteria in conjunction with the reduction of Firmicutes and Bacteroidetes in the Ab-NH group. However, our data suggest that such modulation in gut microbiota would have limited effects on obesity-mediated increment of gut leakage as well as endotoxemia. Nevertheless, future studies are required to reveal the extent to which Proteobacteria modulate changes in the systemic energy homeostasis in response to V + B in DIO.

Various biological pathways facilitate the crosstalk between host energy homeostasis and gut microbiota. Here,

our data suggest that V + B-induced alteration of gut microbiota modulates insulin sensitivity by promoting GLP-1 secretion. GLP-1 is a gut hormone mainly secreted from L-cells in the gut in response to nutrient status (18, 40). Particularly, the active form of GLP-1 (7-36 amide) governs systemic energy homeostasis by regulating satiety in brain, insulin secretion in pancreatic islets, and glucose uptake in muscle (59). Although a previous report has shown that GLP-1 secretion is reduced in patients with type 2 diabetes (60), the dynamics of GLP-1 secretion in non-diabetic obese rodent models have not been well documented. In Fig. 5B, the level of active GLP-1 in the NH group was lower than that in the NC group. Notably, treatment of Ex(9-39) aggravated glucose intolerance in

diabetes are shown. These metabolites only increased in the Ab-NH group. CE-time-of-flight/MS scans of cationic and anionic metabolites covered a 50–1000 *m/z* range. The Y-axis represents the relative peak area [metabolite peak area/(internal standard peak area × sample amount) or (measured value – theoretical value)/(measured value × 10⁶) in the case of putative metabolites] converted to log₂ ratio. F, G) The levels of GLP-1 in conditioned media. F) NCI-H716 cells were treated with TCA or putrescine or creatine for 2 hours. G) NCI-H716 cells were either treated with TCA and H-89 alone or together. Each bar represents the mean ± SE of the individual samples. ***P* < 0.01.

Ab-NH group, indicating the significance of GLP-1-mediated beneficial effects on energy metabolism in the improvement of glucose intolerance in the Ab-NH group. Previous studies showed that several kinds of prebiotics stimulate GLP-1 secretion and that gut microbiota acts as a mediator by fermenting indigestible prebiotics to short chain fatty acids (61, 62). Consequently, short chain fatty acids induce GLP-1 release from L-cells and modulate systemic energy homeostasis (21). Here, we demonstrated that depletion of Firmicutes and Bacteroidetes in DIO increased production of gut-derived metabolites including TCA, creatine, and protein tyrosine phosphatase 1B. In consistent with previous studies demonstrating that TCA stimulates GLP-1 secretion in humans (51, 63), TCA treatment promoted GLP-1 secretion in L-cells. Thus, findings both in our results and from those human data suggest that an increase in TCA after depletion of Firmicutes and Bacteroidetes would be associated with GLP-1-dependent amelioration of insulin resistance in DIO. In addition to TCA, other metabolites have been reported to have beneficial effects on host energy metabolism (42–46, 48, 49). For instance, sulfotyrosine represses protein tyrosine phosphatase 1B and contributes to the regulation of insulin signaling (45) and creatine is linked with increased GLUT4 expression in muscle (43). Therefore, it is of particular interest to investigate the potential roles of these metabolites in the alleviation of insulin resistance mediated by alteration of Firmicutes and Bacteroidetes in DIO in the future.

In this study, the serum insulin levels of the Ab-NH group were lower than those in the NH group in food withdrawal and feeding conditions, implying that alternative mechanisms might enhance insulin sensitivity, independent of active GLP-1-mediated stimulation of insulin release. In the pancreas, active GLP-1 (7-36 amide) binds to GLP-1 receptor to activate PKA signaling, induces insulin secretion, and promotes β -cell survival (40). However, after secretion into the blood, active GLP-1 is rapidly degraded into the inactive GLP-1 (9-36 amide) metabolite within 1–2 min by dipeptidyl peptidase IV (64). Although the role of inactive GLP-1 in glucose metabolism is still unclear, it has been recently suggested that inactive GLP-1 may be involved in the regulation of glucose homeostasis (65, 66). For instance, inactive GLP-1 alone lowers the blood glucose level in anesthetized pigs (65). In dogs, inactive GLP-1 significantly increases myocardial glucose uptake with dilated cardiomyopathy (66). Furthermore, inactive GLP-1 is highly stable in blood, which would prolong the effects of active GLP-1 to improve insulin resistance (51). These findings are consistent with our data that an increment of insulin sensitivity in V + B-treated DIO mice is potentially attributable to increased levels of both active and inactive forms of GLP-1.

Increased adipose tissue inflammation correlates with insulin resistance in obese individuals. Moreover, depletion or aggravation of gut microbiota with various antibiotics alleviates insulin resistance and obesity by reducing inflammatory responses (9, 67). In this study, adipose tissue and whole-body inflammation were similar between NH and Ab-NH groups. However, in a recent study, mice treated with subtherapeutic levels of antibiotics displayed increased adiposity and insulin resistance with subtle but significant changes in gut microbiota (68).

These conflicting results might be derived from the selection and concentration of antibiotics, which would influence metabolic changes and adipose tissue dysregulation.

In conclusion, we demonstrated that alteration of gut microbiota, with significant depletion of Firmicutes and Bacteroidetes, by treatment with V + B would improve insulin resistance in DIO mice. Apparently, such modulation in gut microbiota alters profiles of gut-derived metabolites and consequently augments GLP-1 secretion. Taken together, these findings may provide an insight into the understanding of biologic mechanisms involved in the regulation of insulin sensitivity in obese subjects. FJ

This work was supported by the National Research Foundation of Korea (2011-0018312), the Korea Institute of Planning & Evaluation for Technology in Food, Agriculture, Forestry and Fisheries (311054-03-HD110), and the Ministry of Science, Information and Communications Technology (ICT) & Future Planning (2012M3A9B6055344). I.H. was supported by the BK21 program and a Hi Seoul Science (Humanities) Fellowship funded by the Seoul Scholarship Foundation. Y.J.P. was supported by the World Class University (WCU) program. The authors also thank Won-Gun Choi, Jong In Kim, and Jin Young Huh for helpful discussions.

REFERENCES

- Ludwig, D. S. (2002) The glycemic index: physiological mechanisms relating to obesity, diabetes, and cardiovascular disease. *JAMA* **287**, 2414–2423
- Christakis, N. A., and Fowler, J. H. (2007) The spread of obesity in a large social network over 32 years. *N. Engl. J. Med.* **357**, 370–379
- Schulz, M. D., Atay, C., Heringer, J., Romrig, F. K., Schwitalla, S., Aydin, B., Ziegler, P. K., Varga, J., Reindl, W., Pommerenke, C., Salinas-Riester, G., Böck, A., Alpert, C., Blaut, M., Polson, S. C., Brandl, L., Kirchner, T., Greten, F. R., Polson, S. W., and Arkan, M. C. (2014) High-fat-diet-mediated dysbiosis promotes intestinal carcinogenesis independently of obesity. *Nature* **514**, 508–512
- Olefsky, J. M., and Glass, C. K. (2010) Macrophages, inflammation, and insulin resistance. *Annu. Rev. Physiol.* **72**, 219–246
- Jo, H., Choe, S. S., Shin, K. C., Jang, H., Lee, J. H., Seong, J. K., Back, S. H., and Kim, J. B. (2013) Endoplasmic reticulum stress induces hepatic steatosis via increased expression of the hepatic very low-density lipoprotein receptor. *Hepatology* **57**, 1366–1377
- Bäckhed, F., Ding, H., Wang, T., Hooper, L. V., Koh, G. Y., Nagy, A., Semenkovich, C. F., and Gordon, J. I. (2004) The gut microbiota as an environmental factor that regulates fat storage. *Proc. Natl. Acad. Sci. USA* **101**, 15718–15723
- Ley, R. E., Bäckhed, F., Turnbaugh, P., Lozupone, C. A., Knight, R. D., and Gordon, J. I. (2005) Obesity alters gut microbial ecology. *Proc. Natl. Acad. Sci. USA* **102**, 11070–11075
- Bäckhed, F., Manchester, J. K., Semenkovich, C. F., and Gordon, J. I. (2007) Mechanisms underlying the resistance to diet-induced obesity in germ-free mice. *Proc. Natl. Acad. Sci. USA* **104**, 979–984
- Cani, P. D., Bibiloni, R., Knauf, C., Waget, A., Neyrinck, A. M., Delzenne, N. M., and Burcelin, R. (2008) Changes in gut microbiota control metabolic endotoxemia-induced inflammation in high-fat diet-induced obesity and diabetes in mice. *Diabetes* **57**, 1470–1481
- Membrez, M., Blancher, F., Jaquet, M., Bibiloni, R., Cani, P. D., Burcelin, R. G., Corthesy, I., Macé, K., and Chou, C. J. (2008) Gut microbiota modulation with norfloxacin and ampicillin enhances glucose tolerance in mice. *FASEB J.* **22**, 2416–2426
- Hildebrandt, M. A., Hoffmann, C., Sherrill-Mix, S. A., Keilbaugh, S. A., Hamady, M., Chen, Y. Y., Knight, R., Ahima, R. S., Bushman, F., and Wu, G. D. (2009) High-fat diet determines the composition of the murine gut microbiome independently of obesity. *Gastroenterology* **137**, 1716–1724, e1–e2

12. Turnbaugh, P. J., Hamady, M., Yatsunenko, T., Cantarel, B. L., Duncan, A., Ley, R. E., Sogin, M. L., Jones, W. J., Roe, B. A., Affourtit, J. P., Egholm, M., Henrissat, B., Heath, A. C., Knight, R., and Gordon, J. I. (2009) A core gut microbiome in obese and lean twins. *Nature* **457**, 480–484
13. Schwirtz, A., Taras, D., Schäfer, K., Beijer, S., Bos, N. A., Donus, C., and Hardt, P. D. (2010) Microbiota and SCFA in lean and overweight healthy subjects. *Obesity (Silver Spring)* **18**, 190–195
14. Collado, M. C., Isolauri, E., Laitinen, K., and Salminen, S. (2008) Distinct composition of gut microbiota during pregnancy in overweight and normal-weight women. *Am. J. Clin. Nutr.* **88**, 894–899
15. Turnbaugh, P. J., Ley, R. E., Mahowald, M. A., Magrini, V., Mardis, E. R., and Gordon, J. I. (2006) An obesity-associated gut microbiome with increased capacity for energy harvest. *Nature* **444**, 1027–1031
16. Van Eldere, J., Celis, P., De Pauw, G., Lesaffre, E., and Eysen, H. (1996) Tauroconjugation of cholic acid stimulates 7 alpha-dehydroxylation by fecal bacteria. *Appl. Environ. Microbiol.* **62**, 656–661
17. Martin, F. P., Dumas, M. E., Wang, Y., Legido-Quigley, C., Yap, I. K., Tang, H., Zirah, S., Murphy, G. M., Cloarec, O., Lindon, J. C., Sprenger, N., Fay, L. B., Kochhar, S., van Bladeren, P., Holmes, E., and Nicholson, J. K. (2007) A top-down systems biology view of microbiome-mammalian metabolic interactions in a mouse model. *Mol. Syst. Biol.* **3**, 112
18. Campbell, J. E., and Drucker, D. J. (2013) Pharmacology, physiology, and mechanisms of incretin hormone action. *Cell Metab.* **17**, 819–837
19. Brubaker, P. L. (2006) The glucagon-like peptides: pleiotropic regulators of nutrient homeostasis. *Ann. N. Y. Acad. Sci.* **1070**, 10–26
20. Pols, T. W. H., Auwerx, J., and Schoonjans, K. (2010) Targeting the TGR5-GLP-1 pathway to combat type 2 diabetes and non-alcoholic fatty liver disease. *Gastroenterol. Clin. Biol.* **34**, 270–273
21. Tolhurst, G., Heffron, H., Lam, Y. S., Parker, H. E., Habib, A. M., Diakogiannaki, E., Cameron, J., Grosse, J., Reimann, F., and Gribble, F. M. (2012) Short-chain fatty acids stimulate glucagon-like peptide-1 secretion via the G-protein-coupled receptor FFAR2. *Diabetes* **61**, 364–371
22. Chun, J., Kim, K. Y., Lee, J.-H., and Choi, Y. (2010) The analysis of oral microbial communities of wild-type and toll-like receptor 2-deficient mice using a 454 GS FLX Titanium pyrosequencer. *BMC Microbiol.* **10**, 101–108
23. Kim, O. S., Cho, Y. J., Lee, K., Yoon, S. H., Kim, M., Na, H., Park, S. C., Jeon, Y. S., Lee, J. H., Yi, H., Won, S., and Chun, J. (2012) Introducing EzTaxon-e: a prokaryotic 16S rRNA gene sequence database with phylotypes that represent uncultured species. *Int. J. Syst. Evol. Microbiol.* **62**, 716–721
24. Lee, Y. S., Li, P., Huh, J. Y., Hwang, I. J., Lu, M., Kim, J. I., Ham, M., Talukdar, S., Chen, A., Lu, W. J., Bandyopadhyay, G. K., Schwendener, R., Olefsky, J., and Kim, J. B. (2011) Inflammation is necessary for long-term but not short-term high-fat diet-induced insulin resistance. *Diabetes* **60**, 2474–2483
25. Kim, K. H., Yoon, J. M., Choi, A. H., Kim, W. S., Lee, G. Y., and Kim, J. B. (2009) Liver X receptor ligands suppress ubiquitination and degradation of LXRA by displacing BARD1/BRCA1. *Mol. Endocrinol.* **23**, 466–474
26. Judex, S., Luu, Y. K., Ozcivici, E., Adler, B., Lublinsky, S., and Rubin, C. T. (2010) Quantification of adiposity in small rodents using micro-CT. *Methods* **50**, 14–19
27. Huh, J. Y., Kim, J. I., Park, Y. J., Hwang, I. J., Lee, Y. S., Sohn, J. H., Lee, S. K., Alfadda, A. A., Kim, S., Choi, S. H., Lee, D. S., Park, S. H., Seong, R. H., Choi, C. S., and Kim, J. B. (2013) A novel function of adipocytes in lipid antigen presentation to iNKT cells. *Mol. Cell. Biol.* **33**, 328–339
28. Matsumoto, M., Kibe, R., Ooga, T., Aiba, Y., Kurihara, S., Sawaki, E., Koga, Y., and Benno, Y. (2012) Impact of intestinal microbiota on intestinal luminal metabolome. *Sci. Rep.* **2**, 233–242
29. Johnson, B. A., Anker, H., Meleney, F. L. (1945) Bacitracin: a new antibiotic produced by a member of the *B. subtilis* group. *Science* **102**, 376–377
30. Wolf, M., Müller, T., Dandekar, T., and Pollack, J. D. (2004) Phylogeny of Firmicutes with special reference to Mycoplasma (Mollicutes) as inferred from phosphoglycerate kinase amino acid sequence data. *Int. J. Syst. Evol. Microbiol.* **54**, 871–875
31. Bacon, A. E., McGrath, S., Fekety, R., and Holloway, W. J. (1991) In vitro synergy studies with *Clostridium difficile*. *Antimicrob. Agents Chemother.* **35**, 582–583
32. Eng, R. H. K., Ng, K., and Smith, S. M. (1993) Susceptibility of resistant *Enterococcus faecium* to unusual antibiotics. *J. Antimicrob. Chemother.* **31**, 609–610
33. Rao, S., Kupfer, Y., Pagala, M., Chapnick, E., and Tessler, S. (2011) Systemic absorption of oral vancomycin in patients with *Clostridium difficile* infection. *Scand. J. Infect. Dis.* **43**, 386–388
34. de La Serre, C. B., Ellis, C. L., Lee, J., Hartman, A. L., Rutledge, J. C., and Raybould, H. E. (2010) Propensity to high-fat diet-induced obesity in rats is associated with changes in the gut microbiota and gut inflammation. *Am. J. Physiol. Gastrointest. Liver Physiol.* **299**, G440–G448
35. Lingohr, M. K., Buettner, R., and Rhodes, C. J. (2002) Pancreatic beta-cell growth and survival—a role in obesity-linked type 2 diabetes? *Trends Mol. Med.* **8**, 375–384
36. Patsouris, D., Li, P. P., Thapar, D., Chapman, J., Olefsky, J. M., and Neels, J. G. (2008) Ablation of CD11c-positive cells normalizes insulin sensitivity in obese insulin resistant animals. *Cell Metab.* **8**, 301–309
37. Permana, P. A., Menge, C., and Reaven, P. D. (2006) Macrophage-secreted factors induce adipocyte inflammation and insulin resistance. *Biochem. Biophys. Res. Commun.* **341**, 507–514
38. Cani, P. D., Amar, J., Iglesias, M. A., Poggi, M., Knauf, C., Bastelica, D., Neyrinck, A. M., Fava, F., Tuohy, K. M., Chabo, C., Waget, A., Delmée, E., Cousin, B., Sulpice, T., Chamontin, B., Ferrières, J., Tanti, J. F., Gibson, G. R., Casteilla, L., Delzenne, N. M., Alessi, M. C., and Burcelin, R. (2007) Metabolic endotoxemia initiates obesity and insulin resistance. *Diabetes* **56**, 1761–1772
39. Petersen, K. F., Dufour, S., Befroy, D., Lehrke, M., Hendler, R. E., and Shulman, G. I. (2005) Reversal of nonalcoholic hepatic steatosis, hepatic insulin resistance, and hyperglycemia by moderate weight reduction in patients with type 2 diabetes. *Diabetes* **54**, 603–608
40. Baggio, L. L., and Drucker, D. J. (2007) Biology of incretins: GLP-1 and GIP. *Gastroenterology* **132**, 2131–2157
41. Ranganath, L. R., Beety, J. M., Morgan, L. M., Wright, J. W., Howland, R., and Marks, V. (1996) Attenuated GLP-1 secretion in obesity: cause or consequence? *Gut* **38**, 916–919
42. Watała, C., Kaźmierczak, P., Dobaczewski, M., Przygodzki, T., Bartuś, M., Łomnicka, M., Stomińska, E. M., Durackova, Z., and Chłopicki, S. (2009) Anti-diabetic effects of 1-methylnicotinamide (MNA) in streptozocin-induced diabetes in rats. *Pharmacol. Rep.* **61**, 86–98
43. Op 't Eijnde, B., Ursø, B., Richter, E. A., Greenhaff, P. L., and Hespel, P. (2001) Effect of oral creatine supplementation on human muscle GLUT4 protein content after immobilization. *Diabetes* **50**, 18–23
44. MacDonald, M. J., and Fahien, L. A. (1988) Glycerinaldehyde phosphate and methyl esters of succinic acid. Two “new” potent insulin secretagogues. *Diabetes* **37**, 997–999
45. Desmarais, S., Jia, Z., and Ramachandran, C. (1998) Inhibition of protein tyrosine phosphatases PTP1B and CD45 by sulfotyrosyl peptides. *Arch. Biochem. Biophys.* **354**, 225–231
46. Rose, W. C. (1911) Mucic acid and intermediary carbohydrate metabolism. *J. Biol. Chem.* **10**, 123–138
47. Kobayashi, M., Ikegami, H., Fujisawa, T., Nojima, K., Kawabata, Y., Noso, S., Babaya, N., Itoi-Babaya, M., Yamaji, K., Hiromine, Y., Shibata, M., and Ogihara, T. (2007) Prevention and treatment of obesity, insulin resistance, and diabetes by bile acid-binding resin. *Diabetes* **56**, 239–247
48. Méndez, J. D., and Balderas, F. (2001) Regulation of hyperglycemia and dyslipidemia by exogenous L-arginine in diabetic rats. *Biochimie* **83**, 453–458
49. Enrique-Tarancón, G., Castan, I., Morin, N., Marti, L., Abella, A., Camps, M., Casamitjana, R., Palacín, M., Testar, X., Degerman, E., Carpené, C., and Zorzano, A. (2000) Substrates of semicarbazide-sensitive amine oxidase co-operate with vanadate to stimulate tyrosine phosphorylation of insulin-receptor-substrate proteins, phosphoinositide 3-kinase activity and GLUT4 translocation in adipose cells. *Biochem. J.* **350**, 171–180
50. Lauffer, L. M., Iakubov, R., and Brubaker, P. L. (2009) GPR119 is essential for oleoylethanolamide-induced glucagon-like peptide-1 secretion from the intestinal enteroendocrine L-cell. *Diabetes* **58**, 1058–1066

51. Wu, T., Bound, M. J., Standfield, S. D., Gedulin, B., Jones, K. L., Horowitz, M., and Rayner, C. K. (2013) Effects of rectal administration of taurocholic acid on glucagon-like peptide-1 and peptide YY secretion in healthy humans. *Diabetes Obes. Metab.* **15**, 474–477
52. Swann, J. R., Want, E. J., Geier, F. M., Spagou, K., Wilson, I. D., Sidaway, J. E., Nicholson, J. K., and Holmes, E. (2011) Systemic gut microbial modulation of bile acid metabolism in host tissue compartments. *Proc. Natl. Acad. Sci. USA* **108**, 4523–4530
53. Muegge, B. D., Kuczynski, J., Knights, D., Clemente, J. C., González, A., Fontana, L., Henrissat, B., Knight, R., and Gordon, J. I. (2011) Diet drives convergence in gut microbiome functions across mammalian phylogeny and within humans. *Science* **332**, 970–974
54. Arumugam, M., Raes, J., Pelletier, E., Le Paslier, D., Yamada, T., Mende, D. R., Fernandes, G. R., Tap, J., Bruls, T., Batto, J. M., Bertalan, M., Borruel, N., Casellas, F., Fernandez, L., Gautier, L., Hansen, T., Hattori, M., Hayashi, T., Kleerebezem, M., Kurokawa, K., Leclerc, M., Levenez, F., Manichanh, C., Nielsen, H. B., Nielsen, T., Pons, N., Poulain, J., Qin, J., Sicheritz-Ponten, T., Tims, S., Torrents, D., Ugarte, E., Zoetendal, E. G., Wang, J., Guarner, F., Pedersen, O., de Vos, W. M., Brunak, S., Doré, J., Antolín, M., Artiguenave, F., Blottiere, H. M., Almeida, M., Brechot, C., Cara, C., Chervaux, C., Cultrone, A., Delorme, C., Denariáz, G., Dervyn, R., Foerstner, K. U., Friss, C., van de Guchte, M., Guedon, E., Haimet, F., Huber, W., van Hylekama-Vlieg, J., Jamet, A., Juste, C., Kaci, G., Knol, J., Lakhdari, O., Layec, S., Le Roux, K., Maguin, E., Mérieux, A., Melo Minardi, R., M'riini, C., Muller, J., Oozeer, R., Parkhill, J., Renault, P., Rescigno, M., Sanchez, N., Sunagawa, S., Torrejon, A., Turner, K., Vandemeulebrouck, G., Varela, E., Winogradsky, Y., Zeller, G., Weissenbach, J., Ehrlich, S. D., Bork, P., and Bork, P.; MetaHIT Consortium. (2011) Enterotypes of the human gut microbiome. *Nature* **473**, 174–180
55. Vijay-Kumar, M., Aitken, J. D., Carvalho, F. A., Cullender, T. C., Mwangi, S., Srinivasan, S., Sitaraman, S. V., Knight, R., Ley, R. E., and Gewirtz, A. T. (2010) Metabolic syndrome and altered gut microbiota in mice lacking Toll-like receptor 5. *Science* **328**, 228–231
56. Suez, J., Korem, T., Zeevi, D., Zilberman-Schapira, G., Thaiss, C. A., Maza, O., Israeli, D., Zmora, N., Gilad, S., Weinberger, A., Kuperman, Y., Harmelin, A., Kolodkin-Gal, I., Shapiro, H., Halpern, Z., Segal, E., and Elinav, E. (2014) Artificial sweeteners induce glucose intolerance by altering the gut microbiota. *Nature* **514**, 181–186
57. Larsen, N., Vogensen, F. K., van den Berg, F. W. J., Nielsen, D. S., Andreasen, A. S., Pedersen, B. K., Al-Soud, W. A., Sørensen, S. J., Hansen, L. H., and Jakobsen, M. (2010) Gut microbiota in human adults with type 2 diabetes differs from non-diabetic adults. *PLoS ONE* **5**, e9085–e9094
58. Bode, C., and Bode, J. C. (2005) Activation of the innate immune system and alcoholic liver disease: effects of ethanol per se or enhanced intestinal translocation of bacterial toxins induced by ethanol? *Alcohol. Clin. Exp. Res.* **29**(11, Suppl), 166S–171S
59. Holst, J. J. (2007) The physiology of glucagon-like peptide 1. *Physiol. Rev.* **87**, 1409–1439
60. Muscelli, E., Mari, A., Casolaro, A., Camastra, S., Seghieri, G., Gastaldelli, A., Holst, J. J., and Ferrannini, E. (2008) Separate impact of obesity and glucose tolerance on the incretin effect in normal subjects and type 2 diabetic patients. *Diabetes* **57**, 1340–1348
61. Cani, P. D., Lecourt, E., Dewulf, E. M., Sohet, F. M., Pachikian, B. D., Naslain, D., De Backer, F., Neyrinck, A. M., and Delzenne, N. M. (2009) Gut microbiota fermentation of prebiotics increases satietogenic and incretin gut peptide production with consequences for appetite sensation and glucose response after a meal. *Am. J. Clin. Nutr.* **90**, 1236–1243
62. Musso, G., Gambino, R., and Cassader, M. (2010) Obesity, diabetes, and gut microbiota: the hygiene hypothesis expanded? *Diabetes Care* **33**, 2277–2284
63. Wu, T., Bound, M. J., Standfield, S. D., Jones, K. L., Horowitz, M., and Rayner, C. K. (2013) Effects of taurocholic acid on glycemic, glucagon-like peptide-1, and insulin responses to small intestinal glucose infusion in healthy humans. *J. Clin. Endocrinol. Metab.* **98**, E718–E722
64. Deacon, C. F., Nauck, M. A., Toft-Nielsen, M., Pridal, L., Willms, B., and Holst, J. J. (1995) Both subcutaneously and intravenously administered glucagon-like peptide I are rapidly degraded from the NH₂-terminus in type II diabetic patients and in healthy subjects. *Diabetes* **44**, 1126–1131
65. Deacon, C. F., Plamboeck, A., Møller, S., and Holst, J. J. (2002) GLP-1-(9-36) amide reduces blood glucose in anesthetized pigs by a mechanism that does not involve insulin secretion. *Am. J. Physiol. Endocrinol. Metab.* **282**, E873–E879
66. Nikolaidis, L. A., Elahi, D., Shen, Y. T., and Shannon, R. P. (2005) Active metabolite of GLP-1 mediates myocardial glucose uptake and improves left ventricular performance in conscious dogs with dilated cardiomyopathy. *Am. J. Physiol. Heart Circ. Physiol.* **289**, H2401–H2408
67. Murphy, E. F., Cotter, P. D., Hogan, A., O'Sullivan, O., Joyce, A., Fouhy, F., Clarke, S. F., Marques, T. M., O'Toole, P. W., Stanton, C., Quigley, E. M., Daly, C., Ross, P. R., O'Doherty, R. M., and Shanahan, F. (2013) Divergent metabolic outcomes arising from targeted manipulation of the gut microbiota in diet-induced obesity. *Gut* **62**, 220–226
68. Cho, I., Yamanishi, S., Cox, L., Methé, B. A., Zavadil, J., Li, K., Gao, Z., Mahana, D., Raju, K., Teitler, I., Li, H., Alekseyenko, A. V., and Blaser, M. J. (2012) Antibiotics in early life alter the murine colonic microbiome and adiposity. *Nature* **488**, 621–626

Received for publication October 19, 2014.

Accepted for publication February 3, 2015.